Proceedings of the ASME 2015 Conference on Smart Materials, Adaptive Structures and Intelligent Systems
SMASIS2015
September 21-23, 2015, Colorado Springs, Colorado, USA

SMASIS2015-8968

SELF-FOLDING LAMINATED COMPOSITES FOR SMART ORIGAMI STRUCTURES

Venkata Siva C. Chillara
Smart Vehicle Concepts Center
The Ohio State University
Columbus, Ohio 43210
Email: chillara.1@osu.edu

Leon M. Headings
Smart Vehicle Concepts Center
The Ohio State University
Columbus, Ohio 43210
Email: headings.4@osu.edu

Marcelo J. Dapino
Smart Vehicle Concepts Center
The Ohio State University
Columbus, Ohio 43210
Email: dapino.1@osu.edu

ABSTRACT

Origami-folding principles can be used with laminated composites to produce lightweight structures that are capable of drastic changes in shape. This paper presents a smart composite that can actively change its crease pattern to fold itself into different rigid shapes and provide a large range of motion. The composite uses a smart material with variable modulus sandwiched between two fiber-reinforced elastomeric skins, one of which is prestressed. Change in modulus of the sandwiched core layer allows prestress in the elastomeric skin to actuate the fold. Unfolding the structure to a flat shape can be accomplished through either embedded or external actuation. Passive composite panels were fabricated for model development and validation. An analytical model was developed based on classical laminate plate theory to study the influence of core modulus, core thickness, and elastomeric skin prestress on the equilibrium curvature of the composite structure. Selected smart materials that provide a change in modulus when stimulated are discussed as candidates for the core layer of the self-folding composite.

INTRODUCTION

Morphing structures present opportunities in various fields of engineering such as aerospace and automotive. In the aerospace industry, morphing airfoil shapes for the design of adaptive wings for aircraft [1] and deployable mechanisms for optimized packaging in spacecraft [2] are the major areas of research. In the automotive industry, morphing addresses the need to switch shape from a low velocity state to a high velocity state. Aerodynamic performance is critical at high speeds whereas other factors like ground clearance and aesthetics are higher priority at low speeds. Daynes and Weaver [3] reviewed morphing structure concepts for automobiles. The challenge in the development of morphing structures has been the design for load bearing capability, while allowing significant changes in shape.

Origami-folding techniques allow large changes in surface area and as such, they could be a very efficient solution for morphing. Zirbel et al. [4] proposed and demonstrated a rigid origami design for deployable solar arrays that uses rigid surfaces as unit cells, backed by a membrane, to create a foldable structure. Application of folding techniques to engineering structures presents a challenge in that the folds and panels must be able to support operational loads. Our interest is to design a continuous rigid structure which is not pre-creased, but can be folded as desired using external stimuli. In particular, the goal is to produce sharp controllable curvatures that act as folds in a structure. Lan et al. [5] demonstrated a shape memory polymer composite hinge that requires an external force for actuation and is heated above its glass transition temperature to return to its memorized position. Simoneau et al. [6] embedded shape memory alloy wire actuators in a flat composite laminate to achieve large flexural deflection; this structure requires a continuous supply of power to hold its shape. Reprogrammable self-folding structures have been developed by Peraza-Hernandez et al. [7] that use a shape memory alloy mesh/film as the actuator. Folding is realized through localized heating of the SMA mesh; the unfolded shape of the structure is recovered upon cooling. The above mentioned designs rely on the configuration of the active material in the composite structure for shape recovery. In this

Copyright © 2015 by ASME

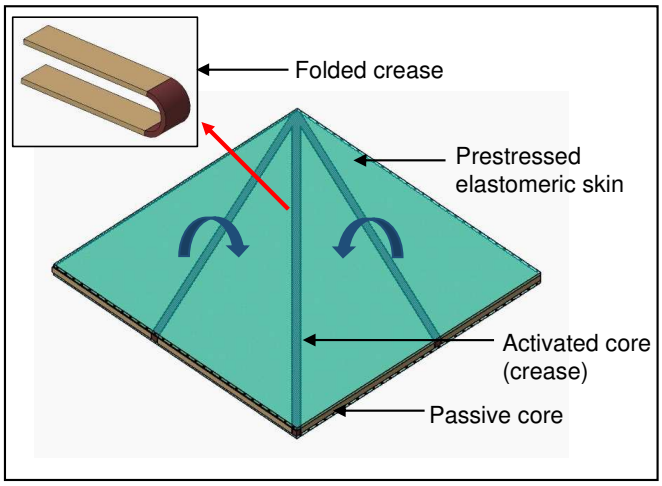

FIGURE 1. SELECTIVE FOLDING OF THE SMART COMPOSITE SHOWN ON AN ORIGAMI KITE BASE.

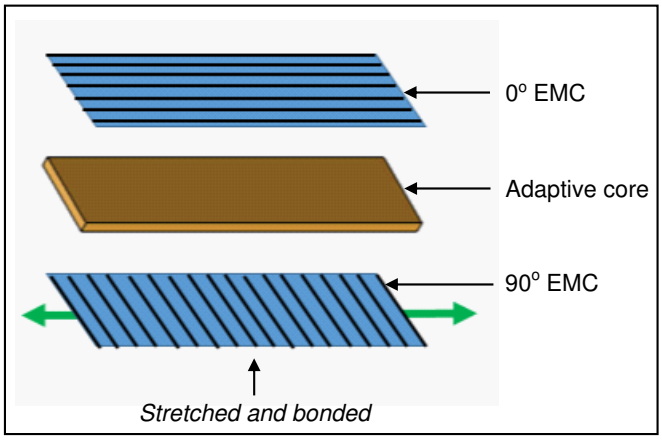

FIGURE 2. SCHEMATIC DIAGRAM SHOWING THE VARIOUS LAYERS OF A SELF-FOLDING COMPOSITE.

scenario, improving the functionality of the passive structure by means of an intrinsic restoring force can have some added benefits: an equilibrium geometry with a prescribed curvature can be realized; higher global stiffness can be achieved for morphing applications; one-way actuation may be sufficient; and actuation power requirements can be minimized.

This paper presents the concept of a smart laminated composite in which controllable folds can be created in a large continuous surface through selective activation of creases (Fig. 1). Creases are defined by a localized change in modulus of the sandwiched core layer; activation energy is supplied by an external source to change the core's modulus. Once the crease is activated, mechanical prestress in one of the elastomeric surface layers drives the composite to fold itself. Upon removal of the external stimulus, the panel can be unfolded using either embedded or external actuators. This smart composite panel can hold various complex folded geometries. Suitable candidates for the active core layer include smart materials such as shape memory alloys, shape memory polymers, magnetorheological elastomers, and paraffin wax. The geometric extent and speed of folding the composite depends on the response of the material used in the core layer. The elastomeric surface layers flex to allow complete folding of surfaces.

The composite structure consists of fiber reinforced elastomeric skins, which are commonly known as elastomeric matrix composites (EMC), placed on opposite faces of the sandwiched core. Fiber reinforcement allows anisotropic stiffness tailoring in elastomeric skins. Peel and Jensen [8] tested and modeled multiple configurations of EMCs consisting of cotton and fiberglass fibers in silicone and urethane rubber media. Bubert et al. [9] developed an EMC skin with unidirectional carbon fibers embedded in silicone rubber for span morphing of an aircraft wing. Due to the restriction provided by the fibers in the lateral direction, this skin exhibits nearly zero Poisson's ratio. The EMC skins are critical design elements in the proposed composite. The following sections describe the concept, modeling, and applicability of the composite to morphing.

SELF-FOLDING COMPOSITE CONFIGURATION

The proposed self-folding composite consists of a variable modulus core layer sandwiched between two EMC skins in orthogonal fiber orientations (Fig. 2). The EMC skins have unidirectional carbon fibers embedded in the 90° and 0° orientations, respectively. The 90° EMC is held with a prescribed prestress while it is bonded to one face of the adaptive core layer. The 0° EMC is then bonded with no prestress to the opposite face of this core. A thin layer of flexible, room temperature vulcanizing (RTV) silicone sealant is used to bond the laminates. Post curing, the composite panel has a uniaxial curvature. A part of the strain energy imparted to the 90° EMC is employed to bend the host structure, defined as the core layer and the 0° EMC. Curvature in the transverse direction can be achieved by prestressing the 0° EMC instead. Thus, a large panel can be folded by prestressing the appropriate EMC skin. A bistable structure may be achieved by prestressing both EMC layers. Since this work is focused on foldable structures, the analysis is restricted to composites with uniaxial curvature based on prestress in the 90° EMC.

Origami designs can be based on planar or curved surfaces as unit cells in a fold. Depending on how prestresses are applied, either of these surface configurations can be achieved. For example, to produce curved surfaces, the passive core's modulus can be designed such that, at equilibrium, the curved surface of the panel has a desired radius. A localized change in modulus in the panel then creates a fold where the neighboring faces are curved

Copyright © 2015 by ASME

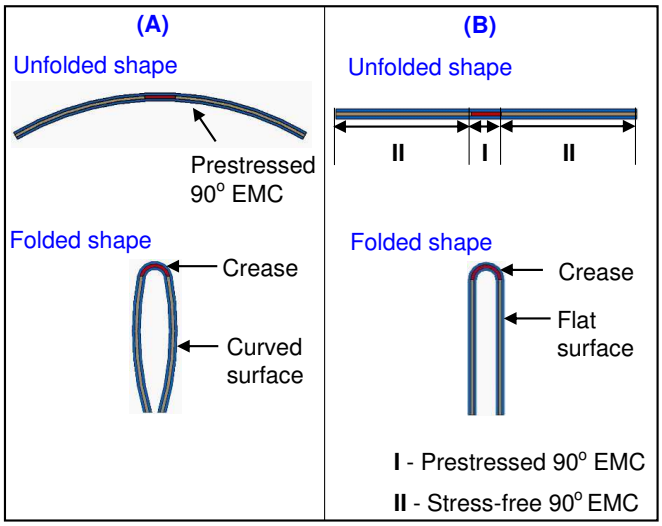

FIGURE 3. A) AN EXAMPLE OF CURVED SURFACES WHEN PRESTRESS IN THE 90° EMC IS UNIFORMLY APPLIED, B) AN EXAMPLE OF FLAT SURFACES WHEN PRESTRESS IN THE 90° EMC IS SELECTIVELY APPLIED.

(shown in Fig. 3(A)). Planar faces can be generated by restricting prestress in the 90° EMC only to the region surrounding a crease (Fig. 3(B)).

COMPOSITE FABRICATION

Composite beam samples are fabricated with a prescribed prestress in the 90° EMC, and their curvatures are measured at equilibrium. The primary step in this process is the fabrication of 90° and 0° EMCs. The following sub-sections describe the fabrication process for the EMC skin and the laminated composite:

EMC Skins

Two layers of unidirectional carbon fibers are wetted with liquid silicone and sandwiched between two pre-cured silicone rubber sheets. The 90° and 0° EMCs have the same design specifications (Table 1) but are used in the matrix dominated and fiber dominated directions, respectively. Rhodorsil 340/CA 45 mold making silicone rubber of durometer grade 45 (shore A) is used as the elastomeric matrix. Unidirectional carbon fibers are prepared by removing transverse fibers from woven carbon fabric (Fiberglast Developments Corp., 3.1 kg/m^2). Through this process, discrete, closely spaced bundles of unidirectional carbon fibers are obtained. Bubert et al. [9] reported poor bonding between carbon fibers and silicone as the reason for deviation of transverse modulus from predictions based on classical laminate plate theory (CLPT). They used commercially available unidirectional carbon fibers, where the fiber bundles are not distinguishable once the binder thread is removed. In contrast, the discrete fiber bundles used in our EMCs fabricated for the self-folding composite appeared to bond well with the matrix while providing near-zero Poisson's ratio (this observation needs further validation). Using the rule of mixtures, the longitudinal (E_L) and transverse (E_T) modulus of a fiber-reinforced composite can be calculated as:

$$E_L = E_f \nu_f + E_m(1-\nu_f), \qquad E_T = \frac{1}{\frac{\nu_f}{E_f} + \frac{1-\nu_f}{E_m}}. \tag{1}$$

For a fiber modulus of 200 GPa and an average matrix modulus of 1.2 MPa (up to 110% strain), the values of E_L and E_T are calculated to be 34 GPa and 1.45 MPa, respectively. A tensile test was conducted on the 90° EMC up to 110% strain with the response shown in Fig. 4. It was found that the measured average transverse elastic modulus of 1.5 MPa agrees well with CLPT predictions in the tested strain range.

TABLE 1. DESIGN DETAILS OF FABRICATED EMC SKINS.

Parameter	Silicone sheet	Carbon fibers	Total
Density (kg/m^3)	1340	53.53	1113
Volume fraction	0.83	0.17	1
Thickness (mm)	0.76 ($\times$ 2)	0.50	2.02

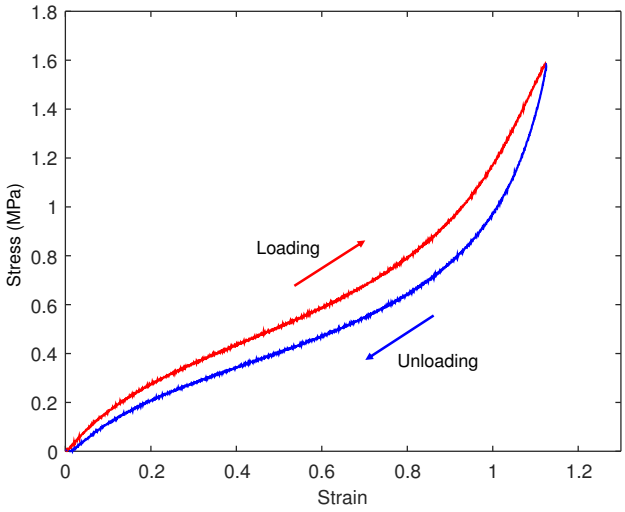

FIGURE 4. STRESS-STRAIN CURVE FOR THE FABRICATED 90° EMC, OBTAINED FROM A UNIAXIAL TENSILE TEST.

Copyright © 2015 by ASME

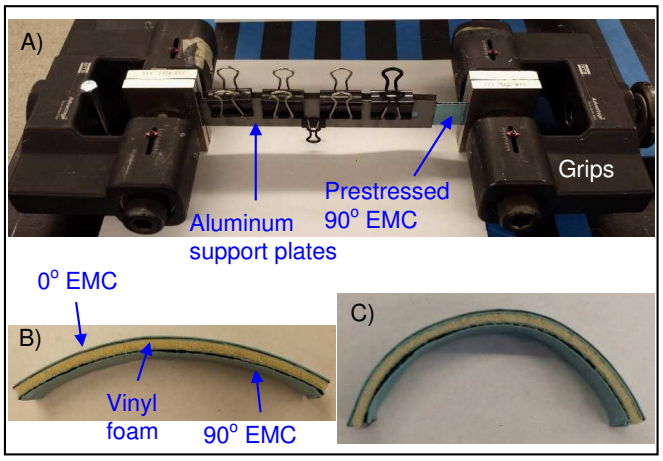

FIGURE 5. A) SETUP FOR CURING THE PRESTRESSED COMPOSITE, B) FINAL COMPOSITE BEAM SAMPLE WITH A PRESTRAIN OF 0.6 IN THE 90° EMC, C) FINAL COMPOSITE BEAM SAMPLE WITH A PRESTRAIN OF 0.8 IN THE 90° EMC.

Laminated Composite Beam

Composite samples were fabricated with vinyl foam as a passive core material to demonstrate the use of prestress in the 90° EMC to produce a curvature in the composite. The selected vinyl foam is an isotropic material that is brittle in nature. However, its flexibility is improved when bonded to a 0° EMC. The 90° EMC is stretched to a given strain and held between a pair of grips (Fig. 5(A)). The three layers are bonded to each other in the configuration shown in Fig. 2 using a silicone adhesive (DAP Auto-Marine 100% RTV silicone sealant) and the bond is allowed to cure at room temperature for 24 hours. Silicone-based adhesives are flexible and compatible with the chosen elastomeric skins and foam layer. After removal from the grips, the resulting composite beam comes to rest in a curved shape that is a function of the prestress imparted to the 90° EMC before bonding. The dimensions of the fabricated beam samples in Fig. 5(B) and Fig. 5(C) are 152.4 × 25.4 × 7.24 (mm). Design parameters for the composite beam are listed in Table 2. The radii of curvature of these samples are reported in the results section.

ANALYTICAL MODEL

The design of the proposed laminated composite is such that it yields a single stable curvature at equilibrium (Fig. 6). A radius of curvature can be calculated as a function of prestress by minimizing the total potential energy of the system using the Rayleigh-Ritz method. Hyer [10], Dano and Hyer [11], and Daynes and Weaver [12], have used this approach to calculate curvatures at equilibrium for laminates with thermally induced bistability. The thermal input applied to a laminated composite is linearly related to strain through the coefficient of thermal

TABLE 2. DESIGN PARAMETERS FOR COMPOSITE BEAM SAMPLES FABRICATED WITH A VINYL FOAM CORE.

Parameter	90° EMC	Core	0° EMC	Composite
Density (kg/m^3)	1113	48	1113	646
Volume fraction	0.28	0.44	0.28	1
Thickness (mm)	2.02	3.175	2.02	7.215
E_x (MPa)	Nonlinear	30	170	-
E_y (MPa)	170	30	1.5	-
ν_{xy}	0	0.33	0	-
ν_{yx}	0	0.33	0	-

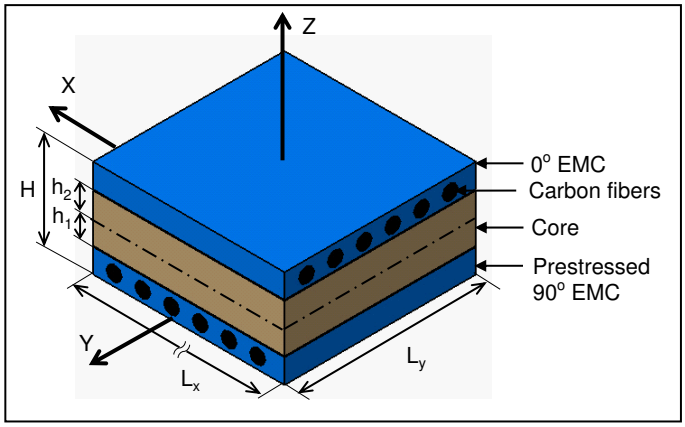

FIGURE 6. GEOMETRY FOR THE LAMINATED COMPOSITE BEAM MODEL.

expansion of the constituent layers. Third degree complete polynomials in x and y were chosen as strain functions to calculate curvature about the X and Y axes and twist in the XY plane. A second degree polynomial in x and y was chosen as the displacement function in the Z direction.

The model presented here involves a similar analytical formulation but uses strain energy in the prestressed 90° EMC as the energy input. Since the 90° EMC layer is designed to have zero Poisson's ratio, curvature about the X axis is neglected. Further, it is assumed that curvature about the X axis due to the differences in the Poisson's ratios between layers is insignificant. The stable shape is expected to be curved about the Y axis such that the prestressed EMC skin is on the concave side. Transverse shear (XZ, YZ) and compressive forces (ZZ) are neglected and a plane stress condition is assumed in this model. Strains for composite materials with geometric nonlinearities based on von

Copyright © 2015 by ASME

Karman's hypothesis [13], as applicable to this problem, are:

$$\varepsilon_{xx} = \frac{\partial u}{\partial x} + \frac{1}{2}\left(\frac{\partial w}{\partial x}\right)^2, \tag{2}$$

$$\varepsilon_{yy} = \frac{\partial v}{\partial y} + \frac{1}{2}\left(\frac{\partial w}{\partial y}\right)^2, \tag{3}$$

$$\gamma_{xy} = \frac{\partial u}{\partial y} + \frac{\partial v}{\partial x} + \frac{\partial w}{\partial x}\frac{\partial w}{\partial y}. \tag{4}$$

Displacements u, v, and w of any point in the composite in the X, Y, and Z directions, respectively, are written in terms of centerline displacements u_0, v_0, and w_0 as:

$$u(x,y,z) = u_0(x) - z\frac{\partial w_0}{\partial x}, \tag{5}$$

$$v(x,y,z) = v_0(y), \tag{6}$$

$$w(x,y,z) = w_0(y). \tag{7}$$

Substitution of (5) - (7) into (2) - (4) yields the strain of an arbitrary plane z of the composite:

$$\varepsilon_{xx} = \frac{\partial u_0}{\partial x} + \frac{1}{2}\left(\frac{\partial w_0}{\partial x}\right)^2 - z\left(\frac{\partial^2 w_0}{\partial x^2}\right), \tag{8}$$

$$\varepsilon_{yy} = \frac{\partial v_0}{\partial y} + \frac{1}{2}\left(\frac{\partial w_0}{\partial y}\right)^2, \tag{9}$$

$$\gamma_{xy} = \frac{\partial u_0}{\partial y} + \frac{\partial v_0}{\partial x} - z\left(\frac{\partial^2 w_0}{\partial y \partial x}\right). \tag{10}$$

Strain of any layer in the composite can be expressed in terms of strain of the geometric centerline as:

$$\varepsilon_x = \varepsilon_x^0 + z\kappa_x^0, \qquad \varepsilon_y = \varepsilon_y^0, \qquad \gamma_{xy} = \gamma_{xy}^0 + z\kappa_{xy}^0 \tag{11}$$

where ε_x^0 and ε_y^0 are the in-plane axial strains, γ_{xy}^0 is the in-plane shear strain, and κ_x^0 and κ_{xy}^0 are the curvature and twist, respectively, of the geometric centerline. Based on existing literature for asymmetric laminates ([10], [11]), the displacement function w in the Z direction can be approximated as:

$$W_0(x) = \frac{1}{2}ax^2, \tag{12}$$

where a represents curvature about the Y axis. The radius of curvature ρ is the reciprocal of a. Strain in the X direction is approximated by a second-degree polynomial in x, which is sufficient to describe curvature in the composite [10]. Since the stress function of the 90° EMC is nonlinear, it is computationally beneficial to restrict the approximation to a second-degree polynomial. Strain in the Y direction is assumed to be a constant. Therefore, the in-plane axial strain of the centerline can be written as:

$$\varepsilon_x^0 = c_0 + c_1 x + c_2 x^2 \quad \text{and} \quad \varepsilon_y^0 = d_0. \tag{13}$$

Shear strain, calculated by integration of (13) to get displacements and substitution into (10), turns out to be zero for this problem. For small in-plane strains, the material behavior in the host structure can be considered to be linear. The 90° EMC, however, must be treated as a nonlinear viscoelastic layer to allow for large prestrain.

Potential Energy Function

The total potential energy (U_T) of the system can be expressed as the sum of strain energy in the host structure and residual strain energy $U^{(90)}$ in the 90° EMC. Neglecting the contribution of the silicone adhesive to the strain energy of the system, one obtains,

$$\begin{aligned} U_T = \int_{-L_x/2}^{L_x/2}\int_{-L_y/2}^{L_y/2}\Bigg\{ & \int_{h_2}^{H/2}\left(\frac{1}{2}Q_{xx}^{(0)}\varepsilon_x^2 + Q_{xy}^{(0)}\varepsilon_x\varepsilon_y + \frac{1}{2}Q_{yy}^{(0)}\varepsilon_y^2\right)\mathrm{d}z \\ & + \int_{-h_1}^{h_2}\left(\frac{1}{2}Q_{xx}^{(c)}\varepsilon_x^2 + Q_{xy}^{(c)}\varepsilon_x\varepsilon_y + \frac{1}{2}Q_{yy}^{(c)}\varepsilon_y^2\right)\mathrm{d}z \\ & + \int_{-H/2}^{-h_1} U^{(90)}\mathrm{d}z\Bigg\}\mathrm{d}y\mathrm{d}x, \end{aligned} \tag{14}$$

where $\{Q_{xx}^{(0)}, Q_{xy}^{(0)}, \text{ and } Q_{yy}^{(0)}\}$ and $\{Q_{xx}^{(c)}, Q_{xy}^{(c)}, \text{ and } Q_{yy}^{(c)}\}$ are the plane stress-reduced stiffness parameters [13] for the 0° EMC and the core layer, respectively,

$$Q_{xx} = \frac{E_x}{1-\nu_{xy}\nu_{yx}}, \quad Q_{xy} = \frac{\nu_{xy}E_y}{1-\nu_{xy}\nu_{yx}}, \quad Q_{yy} = \frac{E_y}{1-\nu_{xy}\nu_{yx}}, \tag{15}$$

where E and ν are the elastic modulus and Poisson's ratio of the layers of the host structure. $U^{(90)}$ is the nonlinear instantaneous strain energy term based on the area under the unloading path of the stress-strain curve for the 90° EMC, which is calculated by integrating stress with respect to strain. The energy associated

Copyright © 2015 by ASME

with unloading is used because it represents the energy transferred to the host structure upon release of prestress after fabrication. The resulting strain energy in the 90° EMC as a function of axial strain of the composite panel is:

$$U^{(90)} = f(\varepsilon_0 - \varepsilon_x). \tag{16}$$

The nonlinear stress function used in the calculation of strain energy in the 90° EMC is described in the following subsection. The equilibrium shape of the morphing structure is obtained by minimization of U_T. Having an exact differential, the potential energy can be written as

$$\begin{aligned}\delta U_T = \left(\frac{\partial U_T}{\partial a}\right)\delta a + \left(\frac{\partial U_T}{\partial c_0}\right)\delta c_0 + \left(\frac{\partial U_T}{\partial c_1}\right)\delta c_1 \\ + \left(\frac{\partial U_T}{\partial c_2}\right)\delta c_2 + \left(\frac{\partial U_T}{\partial d_0}\right)\delta d_0 = 0.\end{aligned} \tag{17}$$

For (17) to hold, each of the partial derivatives of U_T with respect to the independent variables must be zero. This yields five nonlinear equations that can be solved numerically using the Newton-Raphson approach (or similar).

Nonlinear Model of a Prestressed EMC

Peel and Jensen [8] studied the response of fiber-reinforced elastomers and developed a nonlinear model that accounts for geometric and material nonlinearities. A similar method is employed to model the response of a 90° EMC, which is similar to that of a pure elastomer. Since strain in a 90° EMC is very large, a linear strain assumption cannot be used. Geometric nonlinearity is removed from the measured response to obtain a stress-strain curve based on linear strain. The nonlinear Lagrange strain relation in the X direction can be written as:

$$e_x^{(90)} = \frac{\partial u}{\partial x} + \frac{1}{2}\left(\frac{\partial u}{\partial x}\right)^2, \tag{18}$$

where $e_x^{(90)}$ is the measured nonlinear strain and u is the axial displacement. The corresponding linear strain relation is:

$$\varepsilon_x^{(90)} = \frac{\partial u}{\partial x}. \tag{19}$$

The linear strain $\varepsilon_x^{(90)}$ is expressed in terms of $e_x^{(90)}$ as:

$$\varepsilon_x^{(90)} = -1 + \sqrt{1 + 2e_x^{(90)}}. \tag{20}$$

TABLE 3. OGDEN COEFFICIENTS FOR THE UNLOADING CURVE (FIG. 4) OF THE FABRICATED 90° EMC.

Coefficient	i = 1	i = 2	i = 3
p_i	0.481	58.19	-17.33
q_i	3.027	0.223	0.764

Using this linear strain, stress is calculated as:

$$\sigma_i = \sigma_{i-1} + E_i(\varepsilon_i - \varepsilon_{i-1}), \tag{21}$$

where E_i is the instantaneous elastic modulus from experimental measurements. The reduced stress-strain data is now fit to an Ogden rubber model [14] for uniaxial loading, which is expressed as:

$$\sigma_x = \sum_{i=1}^{n} p_i((1+\varepsilon_x)^{(q_i-1)} - (1+\varepsilon_x)^{(-q_i/2-1)}), \tag{22}$$

where p_i and q_i are Ogden coefficients which can be determined by curve fitting uniaxial test data. Three sets of coefficients (n = 3) are found to be sufficient to represent the material nonlinearity of a 90° EMC. Table 3 lists the six Ogden coefficients corresponding to the unloading part of the stress-strain curve of the 90° EMC shown in Fig. 4.

Substituting strain functions described by (11) into (22) and subsequently integrating (22) to find the strain energy of the 90° EMC is computationally expensive. Instead, a quartic polynomial, which accurately replicates the Ogden fit, is used in this model. The equivalent quartic polynomial is:

$$\sigma_x = -0.204{\varepsilon_x}^4 + 1.054{\varepsilon_x}^3 - 1.321{\varepsilon_x}^2 + 1.272\varepsilon_x + 0.025. \tag{23}$$

RESULTS AND DISCUSSION

The unknown polynomial coefficients $\{a, c_0, c_1, c_2, d_0\}$ of the strain functions are calculated by solving the system of nonlinear equations obtained from (17). The material parameters used in this model are obtained from tests carried out on the fabricated samples, as listed in Table 2. The longitudinal modulus (E_x) for the 0° EMC calculated using (1) cannot be used with this model since the fiber and the matrix do not undergo the same amount of in-plane strain. Since the modulus of silicone is much lower than that of carbon fiber, most of the in-plane strain in the 0° EMC occurs in the silicone matrix. The limiting value of stress in the 0° EMC is the shear strength of the fiber-matrix bond, which is used as the effective E_x in the model. This E_x is

Copyright © 2015 by ASME

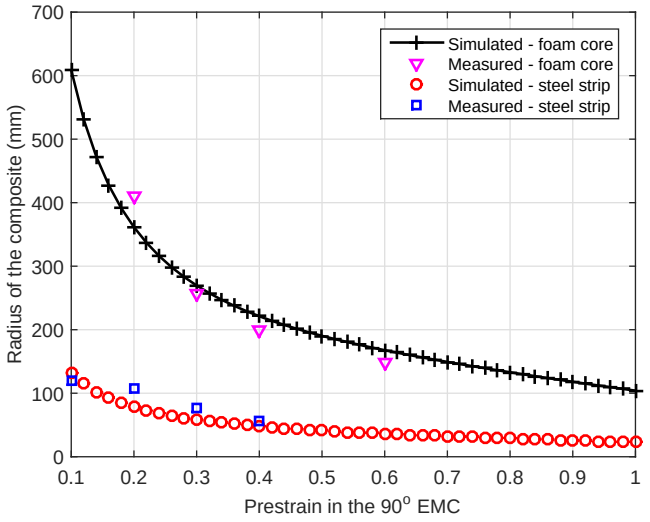

FIGURE 7. RADIUS OF CURVATURE OF THE COMPOSITE VS. PRESTRAIN IN THE 90° EMC.

measured in a uniaxial tensile test where a specimen is mounted in clamping grips and stretched until the fibers slip within the matrix. The average measured shear strength between the fibers and the matrix in the 0° EMC is 170 MPa. The radius of curvature of the fabricated samples is calculated using the measured values of sagitta (s) and chord length ($2L$) as:

$$\rho = \frac{L^2 + s^2}{2s}. \tag{24}$$

Measured radii of composite samples fabricated with various values of prestrain correlate well with model predictions (Fig. 7). In a sample fabricated with a prestrain of 0.8, failure was observed in the vinyl foam layer. This may be due to excessive flexure; the beam is bent almost into a semicircle for an applied prestrain of 0.8 in the 90° EMC. To validate the model, additional composite beam samples with a different layer configuration were fabricated. The 0° EMC is eliminated and a steel strip (4130 alloy) with a thickness of 0.127 mm and a modulus of 200 GPa is bonded to the prestressed 90° EMC. In this case, a prestrain of 0.4 in the 90° EMC results in an approximately semicircular equilibrium shape. The radii of the samples fabricated with the steel strip correlate well with model predictions, as shown in Fig. 7.

CANDIDATE MATERIALS FOR THE ACTIVE CORE

As discussed previously, folding in the composite panel can be achieved through a change in the modulus of its core layer. A wide range of active materials can be employed as the variable modulus core. Possible material options are briefly discussed in this section.

Shape Memory Alloys

Shape memory alloys (SMA) exhibit two different microstructures depending on temperature and stress state. The change in microstructure results in a change in modulus. Commercially available NiTi SMAs have an elastic modulus in the range of 28 to 41 GPa in their low temperature martensite phase and 75 to 83 GPa in their high temperature austenite phase [15]. Since modulus change is accompanied by a strain (up to 8%), they also serve as actuation materials. SMAs in the form of wires, ribbons, or sheets can be directly used as the core or can be embedded in a host material as part of a composite core. The SMA may be used in tension, if offset from the neutral plane, or bending. When the SMA core is martensitic, the prestress in the 90° EMC strains the SMA and folds the crease. Heating the SMA to its austenite phase actuates the structure back to its flat geometry and provides shape fixity because of the higher modulus of austenite.

Shape Memory Polymers

Shape memory polymers (SMP) are capable of a large recoverable deformation when subjected to a thermomechanical cycle. SMPs are stiff below their glass transition temperature (T_g) and are relatively soft above T_g. In their soft state, the shape of the structure can be easily altered, which can then be fixed by cooling the SMP below T_g. Upon re-heating the SMP, the original shape is recovered. The nominal modulus of a typical polystyrene SMP is reported to be around 1.2 GPa above T_g and 2 to 10 MPa below T_g [16]. Flexible foam like materials saturated with SMP can function as an active core. Localized heating of the SMP core allows the prestress in the 90° EMC to actuate the fold. The folded shape can then be fixed by cooling the core below T_g. Upon reheating to soften the same crease, the original unfolded shape can be recovered using an embedded or external actuator and fixed in the unfolded shape by cooling the crease below T_g.

Magnetorheological Materials

Magnetorheological (MR) composites are a class of smart materials whose material property can be controlled by an external magnetic field. They are made up of magnetic particles dispersed in foam, fabric, or elastomeric media. The effective modulus of the composite increases with an increase in the applied magnetic field. Modulus change varies greatly depending on the matrix material, volume fraction of iron particles, and whether the particles are aligned or randomly dispersed. In MR elastomers containing 30% v/v of iron particles, modulus change is

Copyright © 2015 by ASME

about 0.5 MPa [17]. When used as the core, the structure can be designed to fold when the MR layer is in its soft state. Embedded or external actuation could be used to unfold the structure in its soft state. Then, a magnetic field could be applied to rigidize the MR layer and maintain the unfolded shape [18]. MR composites would be most suitable for the folding of soft structures where large deformation is preferred over load bearing capability.

Phase Change Materials

Phase change materials such as paraffin wax are materials whose modulus can be altered through solid-liquid phase transformation. A thin layer of paraffin wax can be encapsulated in a flexible walled chamber to constitute the core layer of the composite. The elastic modulus of paraffin wax in its solid phase is around 250 MPa [19]. Melting the wax results in a reduction in modulus of up to two orders of magnitude, allowing the prestress in the 90° EMC to fold the crease. The composite can be unfolded using either embedded or external actuation and either shape can be fixed by cooling the wax to its solid phase.

PARAMETRIC STUDY: DESIGN OF THE ACTIVE CORE

In this section, the design parameters for the core layer that affect the geometry of the self-folding composite are studied. Suitable active materials previously introduced are identified for a desired radius range of the composite. The geometry of the unfolded composite and the extent of its folding are jointly influenced by the modulus and thickness of the active core.

Effect of Core Modulus Change

For a constant core thickness of 0.127 mm (0.005 in), a modulus sweep is conducted at three different values of prestrain in the 90° EMC to obtain a range for the radius of the composite (Fig. 8). It is assumed that the core material is isotropic. The modulus range considered is 1 MPa to 80 GPa. The lower end of core modulus (up to 1.2 GPa) is plotted on a linear scale and the higher end is plotted on a logarithmic scale for an appropriate illustration of the change in radius. The modulus ranges for some of the active materials previously discussed are indicated to illustrate their ability to fold the composite. It is seen that the variation of composite radius for a given change in core modulus (slope) is higher when the prestrain in the 90° EMC is lower. The radius of the folded composite, corresponding to the lower modulus limit for each active material, is also influenced by the stiffness of the 0° EMC that is bonded to the opposite face of the sandwiched core.

Effect of Core Thickness

Thickness of the core is an important design parameter since it provides insight into the use of different geometric configurations of active materials like thin strips, wires, and thick laminates. Fig. 9 is a contour plot of the radius of the composite plotted as a function of thickness and modulus of the core. The value of prestrain in the 90° EMC is 1.0. This plot serves as a sizing chart for the core, once a suitable active material is chosen. For example, for an unfolded radius of 800 mm, an SMP

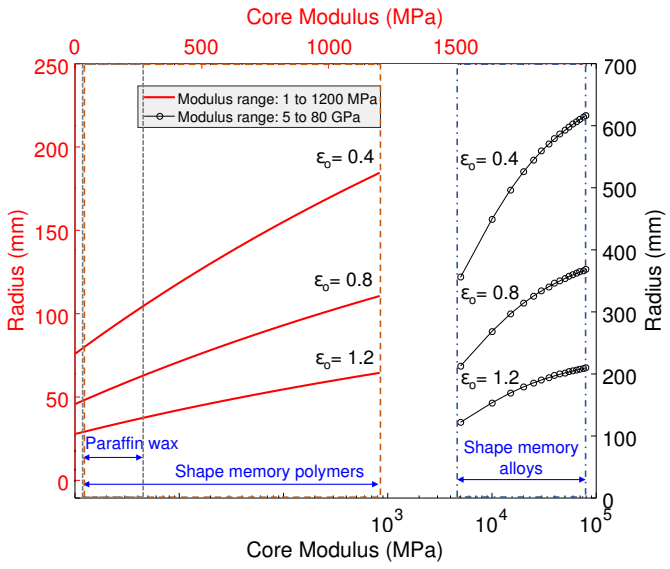

FIGURE 8. RADIUS OF THE COMPOSITE VS. CORE MODULUS FOR A CORE THICKNESS OF 0.127 MM (0.005 IN) AND PRESTRAINS IN THE 90° EMC OF 0.4, 0.8, AND 1.2.

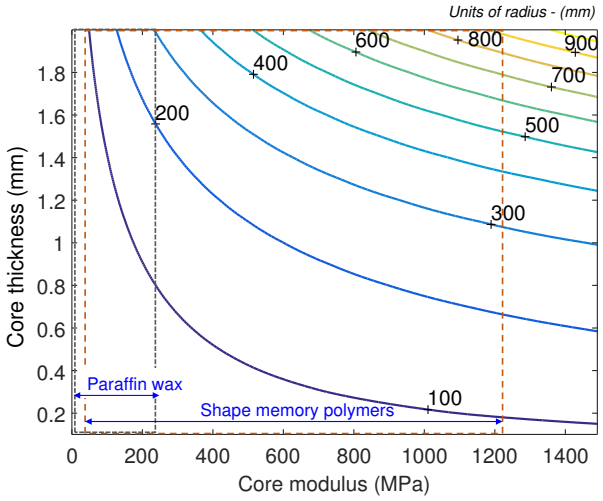

FIGURE 9. CONTOUR PLOT OF THE RADIUS OF THE COMPOSITE VS. CORE MODULUS AND CORE THICKNESS, FOR A PRESTRAIN OF 1.0 IN THE 90° EMC.

Copyright © 2015 by ASME

layer of thickness 1.9 mm can be used to obtain a fold having a radius of around 50 mm. In the case of very stiff active materials like SMAs, the effective modulus of the layer can be reduced by embedding SMA wires or strips in a passive matrix in order to design a composite core layer of appreciable thickness.

SUMMARY AND FUTURE WORK

Self-folding composites, when structurally rigid, are attractive for morphing structures. The presence of an intrinsic restoring force in the passive structure of a smart morphing panel presents the opportunity to design curved panels with tailored stiffness that perform the morphing function without a support structure. The radius of the composite is predicted fairly well by an analytical model that includes the nonlinear behavior of the prestressed EMC. Because morphing in vehicular structures requires the panel to be soft only during shape change, a broad range of active materials that are capable of modulus change are candidates for the core layer. Some of these materials also possess inherent actuation capabilities and could be designed as embedded actuators that unfold the panel. Future work includes the design of a fully controllable self-folding composite for structural morphing applications. The current analytical model will be extended to incorporate a smart material model for an active core layer.

ACKNOWLEDGMENT

Financial support was provided by member organizations of the Smart Vehicle Concepts Center, a National Science Foundation Industry/University Cooperative Research Center (www.SmartVehicleCenter.org). Additional support for S.C. was provided by a Smart Vehicle Center Graduate Fellowship. Technical advice was provided by Dr. Umesh Gandhi, Mr. Hiroyuki Nakatani, and Mr. Kazuhiko Mochida from Toyota Technical Center (TEMA-TTC) in Ann Arbor, MI.

REFERENCES

[1] Barbarino, S., Bilgen, O., Ajaj, R. M., Friswell, M. I., and Inman, D. J., 2011. "A review of morphing aircraft". *Journal of Intelligent Material Systems and Structures,* ***22***(9), pp. 823–877.

[2] Schenk, M., Viquerat, A. D., Seffen, K. A., and Guest, S. D., 2014. "Review of inflatable booms for deployable space structures: Packing and rigidization". *Journal of Spacecraft and Rockets,* ***51***(3), pp. 762–778.

[3] Daynes, S., and Weaver, P. M., 2013. "Review of shape-morphing automobile structures: Concepts and outlook". *Proceedings of the Institution of Mechanical Engineers, Part D: Journal of Automobile Engineering,* ***227***(11), pp. 1603–1622.

[4] Zirbel, S. A., Lang, R. J., Thomson, M. W., Sigel, D. A., Walkemeyer, P. E., Trease, B. P., Magleby, S. P., and Howell, L. L., 2013. "Accommodating thickness in origami-based deployable arrays". *Journal of Mechanical Design,* ***135***(11), p. 111005.

[5] Lan, X., Liu, Y., Lv, H., Wang, X., Leng, J., and Du, S., 2009. "Fiber reinforced shape-memory polymer composite and its application in a deployable hinge". *Smart Materials and Structures,* ***18***(2), p. 024002.

[6] Simoneau, C., Terriault, P., Lacasse, S., and Brailovski, V., 2014. "Adaptive composite panel with embedded SMA actuators: Modeling and validation". *Mechanics Based Design of Structures and Machines,* ***42***(2), pp. 174–192.

[7] Peraza-Hernandez, E., Hartl, D., Galvan, E., and Malak, R., 2013. "Design and optimization of a shape memory alloy-based self-folding sheet". *Journal of Mechanical Design,* ***135***(11), p. 111007.

[8] Peel, L. D., and Jensen, D. W., 2000. "Nonlinear modeling of fiber-reinforced elastomers and the response of a rubber muscle actuator". *Papers-American Chemical Society Division of Rubber Chemistry*(30).

[9] Bubert, E. A., Woods, B. K., Lee, K., Kothera, C. S., and Wereley, W. M., 2010. "Design and fabrication of a passive 1d morphing aircraft skin". *Journal of Intelligent Material Systems and Structures,* ***21***(17), pp. 1699–1717.

[10] Hyer, M. W., 1982. "The room-temperature shapes of four-layer unsymmetric cross-ply laminates". *Journal of Composite Materials,* ***16***(4), pp. 318–340.

[11] Dano, M. L., and Hyer, M. W., 1998. "Thermally-induced deformation behavior of unsymmetric laminates". *International Journal of Solids and Structures,* ***35***(17), pp. 2101–2120.

[12] Daynes, S., and Weaver, P., 2010. "Analysis of unsymmetric CFRP–metal hybrid laminates for use in adaptive structures". *Composites Part A: Applied Science and Manufacturing,* ***41***(11), pp. 1712–1718.

[13] Reddy, J. N., 1997. *Mechanics of Laminated Composite Plates - Theory and Analysis*. Boca Raton, FL: CRC Press.

[14] Ogden, R. W., 1972. "Large deformation isotropic elasticity - on the correlation of theory and experiment for incompressible rubberlike solids". *Proceedings of the Royal Society of London. A. Mathematical and Physical Sciences,* ***326***(1567), pp. 565–584.

[15] Jani, J. M., Leary, M., Subic, A., and Gibson, M. A., 2014. "A review of shape memory alloy research, applications and opportunities". *Materials & Design,* ***56***, pp. 1078–1113.

[16] Leng, J., Lan, X., Liu, Y., and Du, S., 2011. "Shape-memory polymers and their composites: Stimulus methods and applications". *Progress in Materials Science,* ***56***(7), pp. 1077–1135.

[17] Jolly, M. R., Carlson, J. D., and Munoz, B. C., 1996. "A model of the behaviour of magnetorheological materials".

Copyright © 2015 by ASME

Smart Materials and Structures, ***5***(5), pp. 607–614.

[18] Glaser, R., Caccese, V., and Shahinpoor, M., 2011. "Development of magneto-rheological fluid composites with rigidification characteristics". *Smart Materials and Structures,* ***20***(4), p. 045018.

[19] DeSain, J., Brady, B. B., Metzler, K. M., Curtiss, T. J., and Albright, T. V., 2009. "Tensile tests of paraffin wax for hybrid rocket fuel grains". *AIAA,* ***5115***, pp. 1–27.

Copyright © 2015 by ASME